Check for updates

Ecology Letters

WILEY

ECOLOGY LETTERS

LETTER

Pervasive Fitness Trade-Offs Revealed by Rapid Adaptation to Shifting Population Densities in Large Experimental Populations of *Drosophila melanogaster*

M. C. Bitter[1] | S. Greenblum[1,2] | S. Rajpurohit[3,4] | A. O. Bergland[1,5] | J. A. Hemker[1] | E. Lappo[1] | N. J. Betancourt[3] | S. Tilk[1] | S. Berardi[3] | H. Oken[3] | P. Schmidt[3] | D. A. Petrov[1,6]

[1]Department of Biology, Stanford University, Stanford, California, USA | [2]DOE Joint Genome Institute, Lawrence Berkeley National Laboratory, Berkeley, California, USA | [3]Department of Biology, University of Pennsylvania, Philadelphia, Pennsylvania, USA | [4]Division of Biological and Life Sciences, School of Arts and Sciences, Ahmedabad University, Ahmedabad, Gujarat, India | [5]Department of Biology, University of Virginia, Charlottesville, Virginia, USA | [6]Chan Zuckerberg Biohub, San Francisco, California, USA

Correspondence: M. C. Bitter (mcbitter@stanford.edu) | P. Schmidt (schmidtp@sas.upenn.edu) | D. A. Petrov (dpetrov@stanford.edu)

Received: 30 July 2025 | **Revised:** 14 January 2026 | **Accepted:** 16 January 2026

Editor: Jonathan M. Chase

Keywords: adaptation | *Drosophila melanogaster* | eco-evolutionary feedbacks | experimental evolution | fluctuating selection | genomics | population density fluctuations | trade-offs

ABSTRACT

Trade-offs are an inherent feature of organismal biology and fundamental to the evolution of natural populations. Here, we use experimental evolution in large, genetically diverse populations of *Drosophila melanogaster* to directly measure the manifestation of trade-offs in response to fluctuating selection on ecological timescales. We first conducted a lab-based selection experiment to quantify a genome-wide signal of fluctuating selection elicited in response to shifting population densities and in the absence of fluctuating abiotic conditions. We then conducted an independent experiment to show that lab-based manipulations of population density can identify loci relevant to selection during population expansion and collapse in an outdoor setting, where multiple biotic and abiotic conditions fluctuate simultaneously. In concert, our data indicate a role of eco-evolutionary feedbacks and generic fitness trade-offs in the maintenance of variation in natural populations and show how a coarse-grained genetic architecture of adaptation can lead to predictable evolutionary change across settings.

1 | Introduction

A fundamental tenet of evolutionary theory is that trait adaptation is restricted by trade-offs: the cost to individual fitness when an advantageous change in one trait occurs at the detriment to another (Roff and Fairbairn 2007; Stearns 1989). Trade-offs often emerge in the context of life-history traits and, consequently, form the basis of the theory of life history evolution (Stearns 1989). A key theoretical implication of trade-offs is that they maintain variation by constraining the simultaneous optimization of traits associated with fitness under different environmental conditions (Charlesworth 1994; Curtsinger et al. 1994; Rose 1982; Stearns 1989).

A fundamental life-history trade-off is the balance between directing energy towards survival or reproduction: periods of stressful environmental conditions favour somatic maintenance at the cost of reproductive investment (Flatt et al. 2013). Evidence of this trade-off is widespread across species (Cole et al. 2024; Johnston et al. 2013; Mérot et al. 2020), and it is

M.C. Bitter, S. Greenblum, S. Rajpurohit, P. Schmidt and D.A. Petrov contributed equally to this study.

© 2026 John Wiley & Sons Ltd.

clearly apparent among populations of *Drosophila melanogaster* inhabiting temperate environments: increased food accessibility and warmer climates during summer spur exponential population growth, followed in winter by harsher conditions and population collapse (Band and Ives 1961; Gleason et al. 2019; Ives 1945). These cyclical boom-bust population dynamics occur over approximately 10 generations and coincide with the evolution of several classic life history traits: increased reproduction (e.g., fecundity, faster developmental rates) is favoured during spring and summer as populations expand, followed by an increase in stress tolerance traits (e.g., desiccation and starvation resistance) throughout the harsh winter and subsequent population collapse (Behrman et al. 2015; Behrman and Schmidt 2022; Boulétreau-Merle et al. 1987). It is indeed possible that trade-offs underpin these patterns of phenotypic evolution, as negative genetic correlations have been quantified between these seasonally evolving reproduction and stress tolerance traits (Behrman et al. 2015; Hiraizumi 1961; Hoffmann and Parsons 1989a, 1989b; Schmidt et al. 2005; Service 1987; Zera and Harshman 2001).

Recent genome-wide sequencing of wild populations, and outbred populations evolved in semi-natural mesocosms, provides further evidence of the role of trade-offs in adaptation across seasons. Specifically, hundreds of independent loci exhibit signatures of selection concurrent to phenotypic evolution. Many of these loci exhibit a molecular hallmark of underlying trade-offs, antagonistic pleiotropy: the allele favoured during one seasonal phase becomes selected against when the environment fluctuates and contrasting traits evolve (Bergland et al. 2014; Bitter et al. 2024; Machado et al. 2021; Rose 1982; Rudman et al. 2022). Interestingly, there is high repeatability in the genomic loci subject to such fluctuating selection across independent bouts of seasonal adaptation, despite differences in the particular environmental conditions in which patterns of evolutionary change have been quantified (e.g., different study years and locales) (Bergland et al. 2014; Bitter et al. 2024; Machado et al. 2021). One hypothesis for this predictability at the genomic level is that the loci responding to selection are not sensitive to specific environmental variables (which can be idiosyncratic across study locales and years), but rather respond more coarsely to the generic and repeatable demographic fluctuations in the system, such as shifts in population density. The observed genomic parallelism may then represent the manifestation of fundamental fitness trade-offs emerging in response to these shifting demographic conditions (via, e.g., generalised stress response pathways) (Battesti et al. 2011; Kültz 2005; Zhu 2016). Rigorously testing this hypothesized role of density fluctuations in the repeatable genomic patterns of seasonal adaptation necessitates isolating these biotic selective forces from the complex suite of abiotic pressures that fluctuate in natural settings.

Here, we tested whether density fluctuations repeatedly drive selection and elicit trade-offs in *D. melanogaster* using two complementary experimental evolution approaches. In our first experiment, we isolated and quantified the impact of shifting population densities on genomic variation in genetically diverse, replicate populations housed in a controlled, indoor environment (Figure 1; Figure S1). The second experiment then directly quantified the relative contribution of density-induced selection and trade-offs to patterns of seasonal adaptation by pairing observations of allele frequency change in an indoor (lab-based) mesocosm with those from an outdoor (field-based) mesocosm, each seeded from the same initial founder population. In concert, our results provide evidence for: (1) strong, parallel selection elicited by changes in population density; (2) genome-wide trade-offs associated with contrasting selective regimes of population expansion and truncation; and (3) relevance of the loci responding to density selection in a controlled, lab-based setting to patterns of adaptation in response to natural environmental fluctuations.

2 | Materials and Methods

2.1 | Experiment 1: Indoor Expansion and Truncation to Elicit Reproduction/Stress Tolerance Trade-Offs

In Experiment 1 we quantified patterns of genomic variation in genetically diverse, replicate populations housed in a controlled, indoor environment throughout nine discrete (non-overlapping) generations of population expansion, and a single bout of population truncation (Figure 1; Figure S1). Our replicate populations were derived from a reconstituted, outbred population initiated from 145 inbred (DGRP) lines and evolution proceeded in four replicate cages (0.6 × 0.6 × 1.2 m) (Figure 1; Supporting Information; Methods; Data File S1). Throughout population expansion food availability in the replicate cages was commensurate with increasing population sizes, generating a selective regime that eliminated the impact of intraspecific competition (e.g., for food or egg laying space) and favoured the reproduction-associated traits expected when resources are abundant, such as fecundity and developmental rate (Behrman et al. 2015). Due to logistical constraints, a random dilution followed by re-continued expansion was initiated at generation 5 (Figure 1; see Supporting Information; Methods). We ensured non-overlapping generations during expansion by allowing each cohort of newly eclosed flies to lay eggs for a period of 24 h, after which the adults were removed from each replicate. The remaining embryos (i.e., subsequent generation of flies) were then left to develop and eclose, a process repeated for a total of nine generations.

Population truncation, initiated after the first four generations of reproduction selection, was aimed to generate strong selection for traits antagonistic to those favoured throughout expansion. Accordingly, all food and water were removed from our replicate cages and the surviving individuals sampled as the replicate populations collapsed. This mirrors the dynamics of a population that has reached, or exceeded, carrying capacity and is faced with a single bout of strong selection for stress tolerance mechanisms over the course of a single generation, such as during an extreme weather event (Baeckens and Donihue 2025; Del Monte-Luna et al. 2004). Notably, while both food and water were removed, we anticipate desiccation resistance to be the primary driver of selection throughout this phase, as desiccation-induced mortality manifests on substantially faster timescales than starvation (e.g., on the order of several hours vs. days to weeks) (Da Lage et al. 1989). Samples for later DNA extraction and estimation of genome-wide allele

14610248, 2026, 3, Downloaded from https://onlinelibrary.wiley.com/doi/10.1111/ele.70363 by University Of Virginia Claude Moore, Wiley Online Library on [25/03/2026]. See the Terms and Conditions (https://onlinelibrary.wiley.com/terms-and-conditions) on Wiley Online Library for rules of use; OA articles are governed by the applicable Creative Commons License

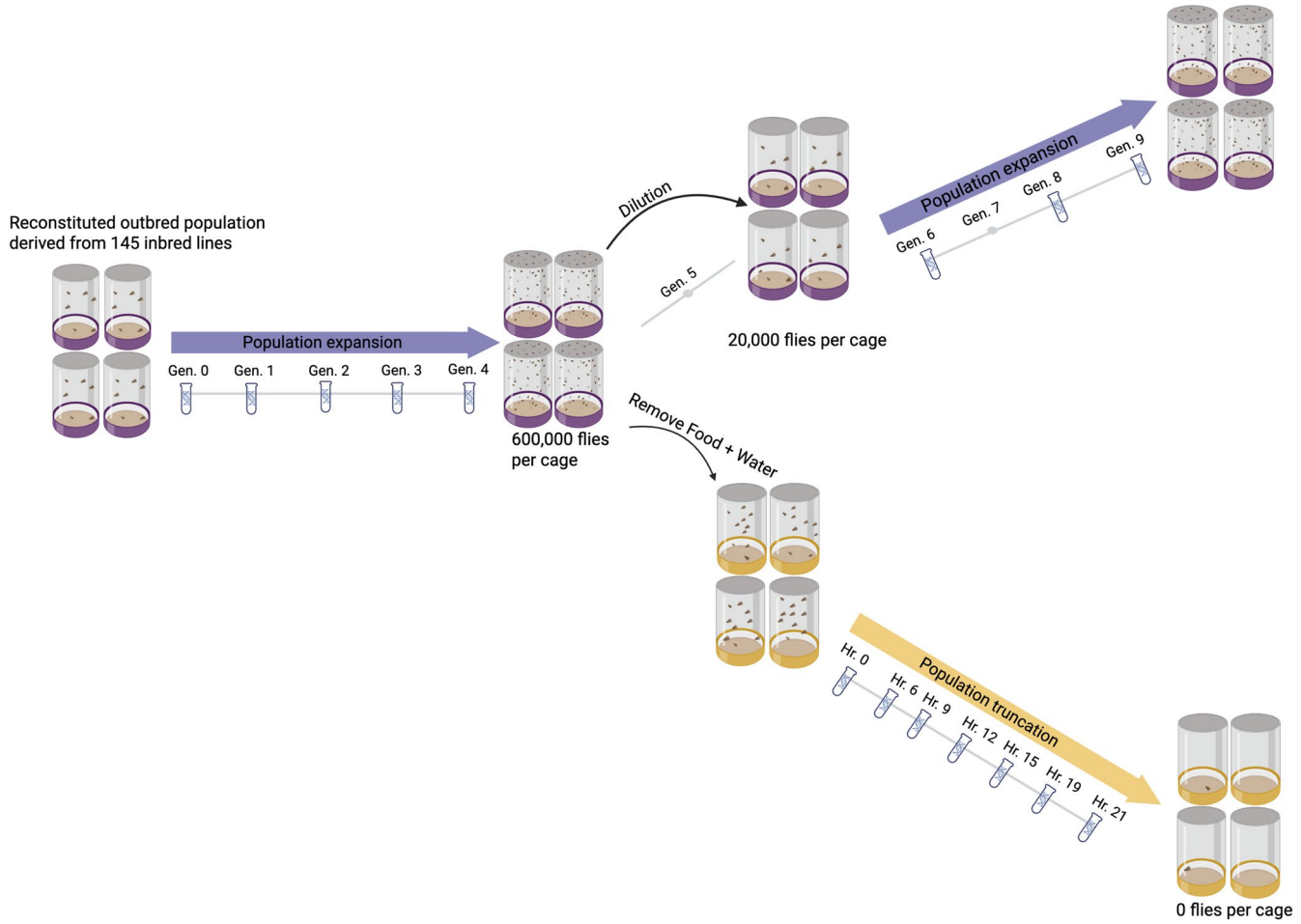

FIGURE 1 | Schematic of Experiment 1. Four replicate, 0.6 × 0.6 × 1.2 m cages were seeded with a genetically diverse, outbred population generated via four generations of recombination ($N = 145$ inbred lines). Evolution proceeded in discrete generations, whereby the amount of food was doubled every generation until replicate populations reached a census size of approximately 600,000 flies per cage (generation four). At this point, eggs from the generation 5 cohort were collected and food and water were removed from the replicate cages. The adult cohort of the generation 4 flies was then sampled at seven time points (h 0–21) as the absence of resources collapsed the populations. The generation 5 eggs were used to re-seed the replicate cages, which underwent continued population expansion for four additional generations. DNA in vials denotes generations of expansion, and hours of truncation, during which pooled samples were collected for pooled allele frequency calculation. Schematic generated with bioRender (https://www.biorender.com/).

frequencies were collected during each of the nine generations of population expansion and at seven time points during population truncation ($N = 100$ males and 100 females per sampling time point and replicate).

2.2 | Experiment 2: Paired Indoor and Outdoor Mesocosm Selection

Our second experiment specifically aimed to quantify whether alleles identified via selection under sustained population expansion in a laboratory setting can predict patterns of adaptation and trade-offs in an outdoor, semi-natural setting. Specifically, during an independent study year we monitored patterns of genomic variation in a genetically diverse, outbred population that was split into a series of large, replicate cages maintained in controlled indoor mesocosms ($N = 10$), as well as outdoor mesocosms exposed to natural environmental fluctuations ($N = 12$). The indoor mesocosms were located in a temperature-controlled laboratory at the University of Pennsylvania (Philadelphia, PA, USA). The outdoor mesocosms were located approximately 1.5 km from this laboratory and comprised replicate cages harbouring a single dwarf peach tree and exposed to natural environmental fluctuations (data generated for the outdoor mesocosm was previously described in Bitter et al. (2024)). The replicate populations inhabiting both mesocosms were seeded with the same genetically diverse, outbred population in June (derived from an inbred reference panel originally collected in local Pennsylvania orchards), and then monitored as they rapidly expanded until reaching carrying capacity after approximately 2 months (see Supporting Information; Methods). Monitoring of the outdoor mesocosms continued throughout the onset of winter, during which time a total crash of the adult populations in the cages was observed. Population-level samples for later DNA sequencing and analysis were collected throughout population expansion in each environment and, for the outdoor mescosms, during the onset of winter and throughout the population collapse ($N = 100$ female flies per sampling time point and replicate).

14610248, 2026, 3, Downloaded from https://onlinelibrary.wiley.com/doi/10.1111/ele.70363 by University Of Virginia Claude Moore, Wiley Online Library on [25/03/2026]. See the Terms and Conditions (https://onlinelibrary.wiley.com/terms-and-conditions) on Wiley Online Library for rules of use; OA articles are governed by the applicable Creative Commons License

2.3 | Sample Sequencing, Allele Frequency Estimation and Statistical Analysis

All samples of pooled flies collected throughout Experiments 1 and 2 were subject to whole genome sequencing. We used the resulting sequencing reads and a local inference method and pipeline to compute high-accuracy, haplotype-informed allele frequency estimates at genome-wide single nucleotide polymorphisms (SNPs) previously identified in our inbred reference panels (Kessner et al. 2013; Tilk et al. 2019). In effect, we retained 1.7 M and 1.9 SNPs across Experiments 1 and 2, respectively, for statistical analysis and inference. Extended detail of the sequencing and bioinformatic pipelines used in the analysis of all sequenced samples is provided in the Supporting Information.

All statistical analyses and data visualisations were carried out using R v.3.5. For samples collected in Experiment 1, we first quantified genome-wide divergence between samples collected during population expansion and truncation using F_{ST}. For both experiments, we identified SNPs with systematic shifts in allele frequencies through time using a generalised linear model. This model assessed the significance of the linear relationship between allele frequency and time of sampling across all cages, using a quasibinomial error model to reduce false positive associations (Wiberg et al. 2017). While an association between allele frequency and sampling timepoint within a single cage may represent either drift or selection, a significant parallel association across all four replicate cages indicates allele frequency trajectories that are parallel across replicate populations. In this case, selection (or linked selection) is the more parsimonious explanation. Accordingly, we used this approach to identify sets of SNPs with signatures of selection and the extent to which the same set of alleles were selected during alternate ecological regimes. Finally, Wright-Fisher simulations in SLiM were implemented to further disentangle the processes underpinning patterns of allele frequency fluctuations observed in our data (Haller and Messer 2023). Additional methodological details for these analyses are provided both in the Results below, as well as our extensive Supporting Information.

3 | Results

3.1 | Lab-Based Population Expansion Elicits Genome-Wide Signals of Strong, Parallel Selection

We observed parallel shifts in allele frequencies across the four replicate populations during Experiment 1's population expansion, indicating adaptive responses to the shared selective pressures imposed in our lab-based system. We quantified these systematic allelic shifts using several approaches. We first computed genome-wide divergence as average F_{ST} across all segregating sites ($N = 1.7$ M SNPs) pairwise among all expansion samples. A linear mixed effects model using these data indicated that F_{ST} divergence from the generation 0 populations increased steadily across cages throughout expansion ($F = 400.97$; $p << 0.001$), though with significant variation in the rate and magnitude of this divergence among individual replicate cages ($F = 6.67$; p-value $= 0.0027$). We next used pairwise F_{ST} values as a distance metric to create multi-dimensional scaling (MDS) plots, in which divergence between samples is represented as distance among the points in a 2-D plane. Colouring samples based on replicate cage identity indicated that genome-wide allele frequencies in one replicate were perturbed, shifting its points from the remaining three replicates throughout expansion (Figure 2B). We suspect this offset to be driven by idiosyncratic selection (i.e., 'batch' effects) imposed upon this replicate prior to sampling, as we did not detect a genomic signature of population bottlenecking that could have similarly given rise to this offset (e.g., genome-wide Tajima's D at the first time point of sampling was near equivalent across samples: 0.253, 0.255, 0.253, 0.255 for replicates 1–4, respectively). Despite this idiosyncratic cage-effect, samples from all replicates shifted across the 2-D MDS plane in the same direction through time, suggesting underlying parallel shifts in genome-wide allele frequencies (Figure 2C, Figure S3; a trend that was also detected using principal component analysis; Figure S4).

We systematically quantified the signature of parallel evolution observed in the two-dimensional MDS space (Figure 2C) by first translating the MDS coordinates for each cage such that the centroid of all generation 0 samples was centered at the origin. We then used these translated points to fit a simple linear regression model to samples from expansion generations 0–4 (Supporting Information; Methods; Figure S5). The resulting axis represents the primary axis of variation in the 2D plane during early expansion for each replicate. We hypothesized that if sustained, directional selection imposed by population expansion was a primary driver of patterns of genomic variation, samples from the remaining expansion generations (generations 6–9) would continue to proceed along the established axis of variation in the same direction. Indeed, projection of late expansion samples onto this axis of variation indicated a significant correlation of sample collection generation and distance along the axis (Figure 2D; Median correlation coefficient across replicates: 0.98; correlation coefficient p-value: 0.03 (derived via $N = 100$ permutations); Table S1). When segregating this analysis by chromosomal arm, however, this parallelism was only evident on chromosomal arms 2L, 3L and 3R. Re-sampling genome-wide SNPs iteratively confirmed that the variation in parallelism across chromosomal arms was not simply due to reduced power on arms with a fewer number of SNPs (Supporting Information; Figure S6, Table S2), and may rather reflect facets of the underlying structure of variation located within these arms (e.g., a lack of chromosomal inversions on X).

To determine the distribution of SNPs contributing to parallel evolution across cages, a generalised linear model (GLM) was fit to allele frequencies across generations 0–9 of expansion. A total of 389,588 SNPs (22.9% of all sites) showed significant parallelism after multiple testing correction (Benjamini-Hochberg false discovery rate < 0.01 and allele frequency change $> 2\%$; Data File S2). These SNPs showed systematic, directional selection across replicates throughout expansion (Figure 2E; Figure S7) and their distribution spanned all five chromosomal arms (Figure 2F). We used a clustering analysis and identified 250 loci as the minimum number of non-overlapping, putatively unlinked targets of selection

14610248, 2026, 3, Downloaded from https://onlinelibrary.wiley.com/doi/10.1111/ele.70363 by University Of Virginia Claude Moore, Wiley Online Library on [25/03/2026]. See the Terms and Conditions (https://onlinelibrary.wiley.com/terms-and-conditions) on Wiley Online Library for rules of use; OA articles are governed by the applicable Creative Commons License

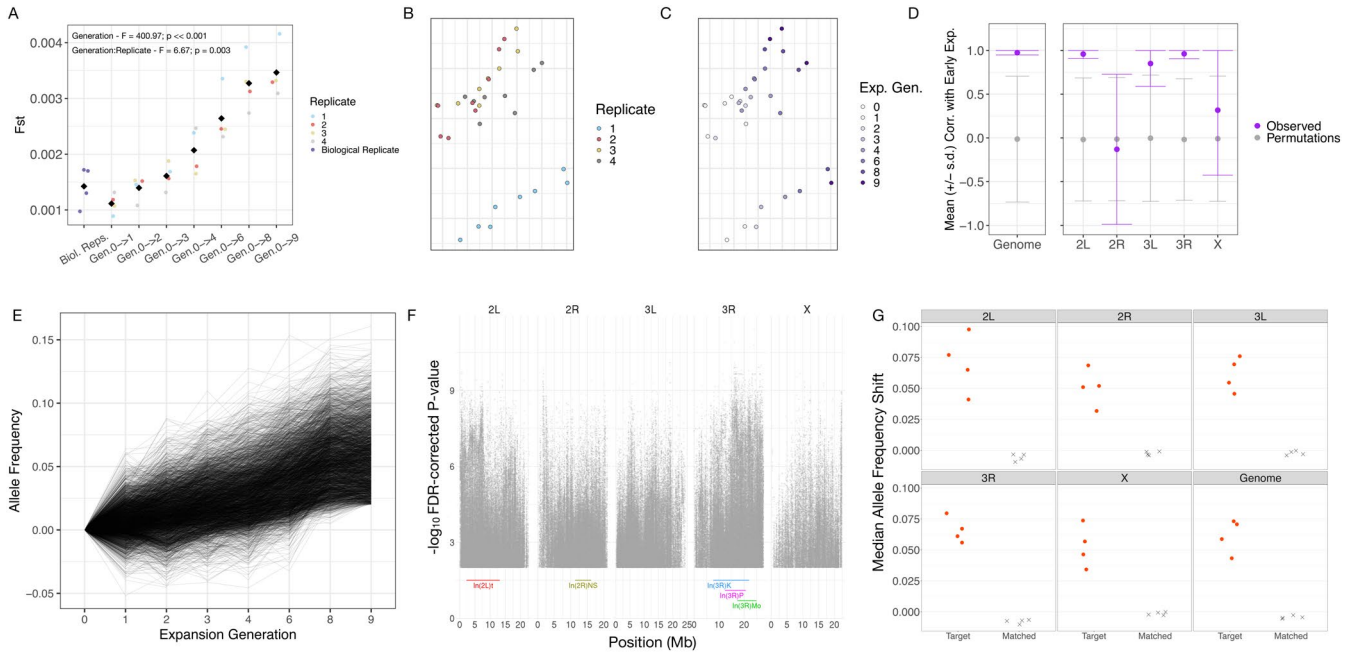

FIGURE 2 | Adaptation under sustained population expansion elicits strong, genome-wide parallel responses. (A) Mean, genome-wide F_{ST} between biological replicates ('Biological Replicates'; same replicate/collection time point, different pooled sample/extraction of flies) and evolved replicate samples and their respective generation 0 expansion sample ('Gen. 0–> *n*'). Faded coloured points indicate individual replicate samples, and black diamonds the average value for each x-axis group. Reported *F* and *p*-values in the top left of the panel result from a linear mixed effects model evaluating the impact of collection generation, and the interaction of replicate and collection generation, on F_{ST} variation throughout the experiment. F_{ST} differentiation from generation 0 samples increased monotonically as function of collection generation ($F = 400.97$; *p*-value < 0.001), and a significant effect of the interaction between collection generation and replicate cage on F_{ST} was observed ($F = 6.67$; *p*-value $= 0.0027$). (B, C) MDS of F_{ST} values computed pairwise across all expansion samples, coloured according to (B) replicate cage or (C) collection generation. (D) Average Pearson Correlation across replicates (+/− standard deviation) between sample expansion generation and distance along a one-dimensional axis constructed using F_{ST} MDS coordinates for early expansion (generation 0–4) samples (C). Purple points and error bars correspond to observed values (mean +/− standard deviation across cages), while grey points and error bars correspond to values derived from $N = 100$ permutations. (E) Trajectories of rising alleles at SNPs identified via GLM (FDR < 0.01 and effect size $> 2\%$) across all nine generations of expansion. (F) Manhattan plot depicting the distribution of SNPs along the genome, as a function of their -$\log_{10}$ FDR-corrected *p*- value derived from a GLM assessing the association of SNP allele frequency and expansion generation. The coordinates of the major cosmopolitan inversions segregating in our founding reference panel at greater than 4% frequency in our founding strains are depicted above the *x*-axis. (G) Leave-one-out cross-validation to infer replicate-level parallelism of adaptation to sustained population expansion. Portrayed is the median shift of the rising allele for sets of target SNPs (points) identified via GLM (FDR < 0.01 and effect size $> 2\%$) in 3 of 4 cages, relative to medians derived from a matched control SNP set (X's), in the fourth replicate. Target SNP medians are coloured red if the distribution of phased allele frequency shifts was significantly greater than that of matched control sites (two-tailed *t*-test, FDR < 0.05).

underpinning this signal (loci ranged in size from 30 to 305 kb) (Data File S3) (Rudman et al. 2022). Quantification of allele frequency trajectories of the most significant SNPs within each locus indicated strong directional selection throughout expansion, with median selection coefficients of 7% per generation (Figure S8). This parallelism was further validated using a leave-one-out cross validation: sets of SNPs identified via GLM in three of the four replicates exhibited a predominantly parallel direction of selection and magnitude of allele frequency change that exceeded background allele frequency movement (quantified using matched control SNPs) in the fourth replicate cage (Figure 2G). While the chromosome-level F_{ST} analysis described above, which focused on signal averaged across all segregating sites, suggested that idiosyncratic behaviour may dominate variation on 2R and X, this analysis demonstrates that there still existed at least some subset of SNPs with parallel allele frequency movement across replicates present on each chromosomal arm.

3.2 | Genomic Evidence of Trade-Offs Induced by Fluctuating Selection Across Population Expansion and Truncation

The parallel frequency shifts observed throughout expansion may be the product of three, not mutually exclusive, evolutionary dynamics: (1) directional selection in response to sustained reproduction selection, (2) adaptation to the lab environment and/or (3) the purging of recessive deleterious alleles (i.e., negative selection) in our outbred population. To disentangle these various dynamics and, in turn, identify the presence of fitness trade-offs at putatively selected alleles, we leveraged our samples collected throughout truncation selection. Specifically, alleles identified during expansion that were a product of consistent lab selection and/or negative selection against unconditionally deleterious recessives should continue to show systematic, directional change throughout truncation (as their effect is not conditional on the specific treatment).

14610248, 2026, 3, Downloaded from https://onlinelibrary.wiley.com/doi/10.1111/ele.70363 by University Of Virginia Claude Moore, Wiley Online Library on [25/03/2026]. See the Terms and Conditions (https://onlinelibrary.wiley.com/terms-and-conditions) on Wiley Online Library for rules of use; OA articles are governed by the applicable Creative Commons License

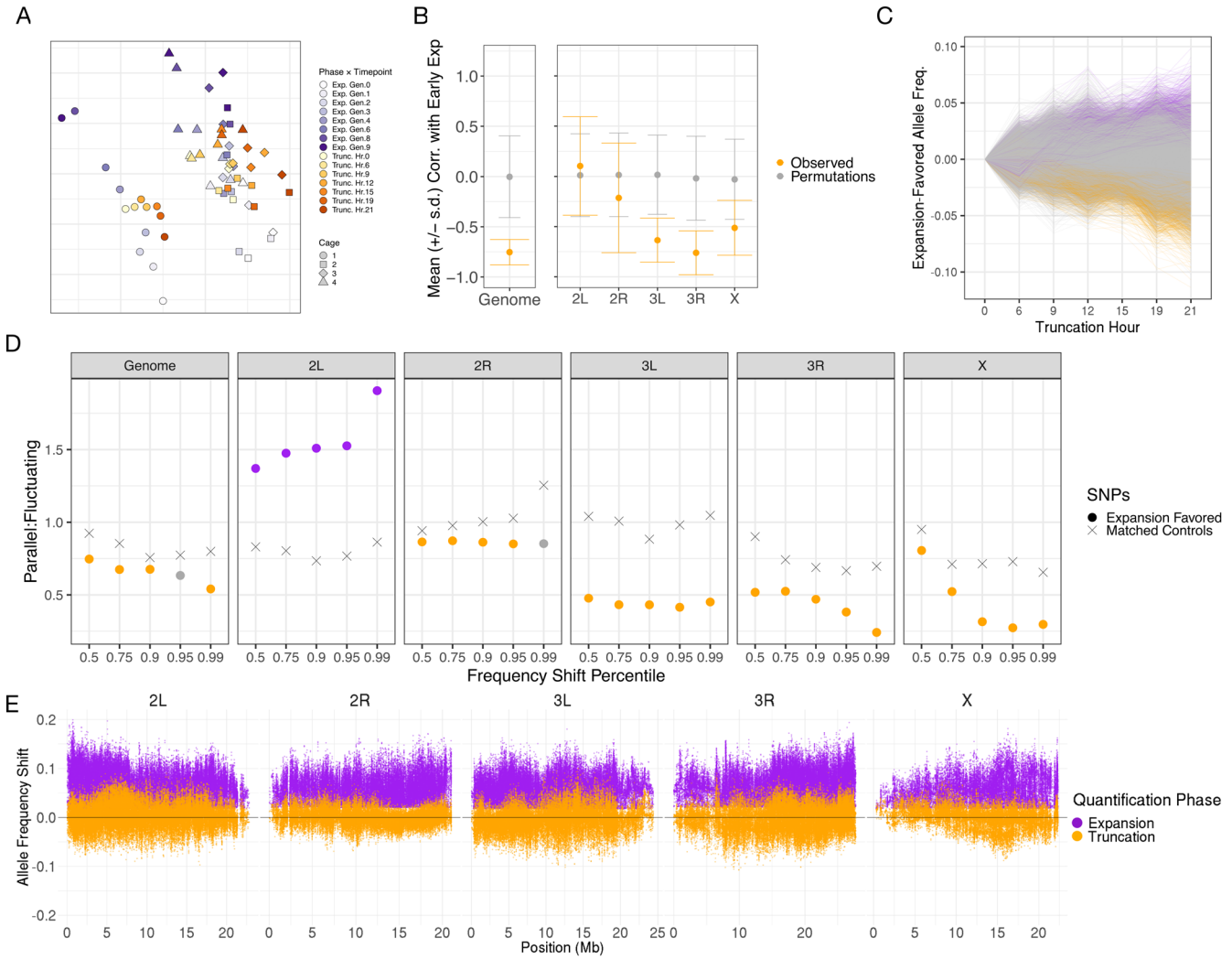

FIGURE 3 | Genome-wide signal of fitness trade-offs between population expansion and truncation. (A) MDS of pairwise F_{ST} values across all samples collected throughout expansion (purple-hue points) and truncation (orange-hue points), shaded according to collection time point (darker hues indicate later expansion or truncation sampling generation/h). (B) Average Pearson correlation across replicates (± standard deviation) between sample expansion generation and distance along a one-dimensional axis constructed using F_{ST} MDS coordinates for early expansion (generation 0–4) samples (A). Orange points and error bars correspond to observed values (mean ± standard deviation across cages), while grey points and error bars correspond to values derived from $N = 100$ permutations. (C) Trajectories of SNPs identified via GLM regression across replicates throughout expansion, measured during truncation. Trajectories are coloured for SNPs that exhibited evidence of systematic allele frequency changes across replicates during truncation (GLM FDR < 0.05 and allele frequency change > 1%) and displayed sustained directional (purple) or fluctuating selection (orange). (D) Ratio of parallel to fluctuating dynamics for expansion-favoured alleles quantified during truncation, segregated by chromosomal arm and percentile of truncation allele frequency shift. Points are further coloured if the ratio of parallel to fluctuating behaviour differed significantly from that expected based on a matched control set (X^2 test p-value < 0.05). (E) Manhattan plot depicting allele frequency shifts throughout expansion (purple points) and truncation (orange points) for alleles increasing in frequency systematically across replicates during expansion.

However, alleles with treatment-specific behaviour during expansion and truncation (i.e., moving in the opposite direction) represent those that likely underpin trade-offs between fecundity and stress tolerance selection.

We initially tested for evidence of context-specific behaviour and trade-offs genome-wide SNPs by re-conducting our MDS analysis of pairwise divergence (F_{st}) values, this time including all samples collected throughout expansion and truncation. If the dominant direction of allele frequency change was sustained across both expansion and truncation (indicating sustained lab selection or purging of deleterious mutations), truncation samples would be ordered from early to late, mirroring the pattern observed for expansion samples (Figure 2B). Instead, we observed that samples taken during truncation shifted back towards earlier expansion samples, suggesting a genome-wide reversion of allele frequencies (Figure 3A; Figure S9). We quantified these trends as above, translating the MDS coordinates of truncation samples such that the centroid of h 0 samples was centered at the origin, and then projected them onto the single axis derived from our linear regression model of early expansion points (Figure 2D; Figure S5). Correlations between collection time and distance along this axis were, genome-wide, significantly negative [Median correlation coefficient across replicates: −0.75, correlation coefficient p-value: 0.01 (derived via $N = 100$

14610248, 2026, 3, Downloaded from https://onlinelibrary.wiley.com/doi/10.1111/ele.70363 by University Of Virginia Claude Moore, Wiley Online Library on [25/03/2026]. See the Terms and Conditions (https://onlinelibrary.wiley.com/terms-and-conditions) on Wiley Online Library for rules of use; OA articles are governed by the applicable Creative Commons License

permutations)], but once again showed heterogeneity among chromosomal arms (Figure 3B; Table S1; Figure S10).

To further resolve the genomic distribution of loci underpinning trade-offs, we interrogated raw allele frequency trajectories. Specifically, we selected those SNPs with GLM-based evidence of selection during expansion and measured the average frequency shifts of the rising allele across replicates throughout truncation. We compared the dynamics of these SNPs to a set of randomly selected, matched control SNPs and found that expansion-favoured SNPs were more likely to become selected against than to be subject to sustained directional selection during truncation ($X^2 = 1123.6$; p-value < 0.001; Figure 3C). We subset this analysis to only those SNPs that displayed evidence of linked selection (via GLM) during both expansion and truncation, finding that fluctuating selection was approximately 3.5 times more likely than sustained directional selection across selection regimes (19,158 fluctuating vs. 5656 directional SNPs). This is visualised in Figure 3D in which we depict the ratio of SNPs with sustained directional, relative to fluctuating, selection. The genomic distribution of sites exhibiting directional or fluctuating behaviour across phases is then depicted in Figure 3E, where for all expansion-favoured alleles we plot separately their allele frequency shift during expansion (purple points) and truncation (orange points).

In the supplement, we show that these patterns of fluctuating selection are in part, but not solely, driven by large and common chromosomal inversions segregating in our study population (Figures S11 and S12, Data Files S4). The Supplement also contains analyses demonstrating the dominant signal in our data to be one of fluctuating selection using empirical cumulative distributions derived from allele frequency trajectories, as well as truncation trajectories of the 250 expansion-identified loci (Figures S13 and S14; Data File S2). Finally, the supplement contains results from an analysis comparing synteny independently for those SNPs identified during expansion and truncation, as well as their propensity to exhibit fluctuating selection across selection regimes (Figures S15 and S16).

It is important to note that our inferences of fluctuating selection reported here are insensitive to the stringency of our filtering criteria, as well as the putative loss/fixation of expansion-selected alleles during truncation (see Supporting Information; Methods Section I.v). Furthermore, our inference of fluctuating selection cannot be a spurious artefact driven by regression to the mean, as the allele frequency data from which the trajectories were computed are entirely independent across expansion and truncation (i.e., share no overlapping time points).

3.3 | One and Two Locus Simulations of Linkage, Selection and Antagonistic Pleiotropy

We explored whether patterns of linkage between loci, antagonistic pleiotropy at a single SNP, and/or haplotype-level antagonistic pleiotropy could generate the patterns of allele frequency change observed in Experiment 1 using Wrigh-Fisher simulations in SLiM (see Supporting Information) (Haller and Messer 2023). We first simulated a scenario in which a single SNP had an advantageous effect on fitness during expansion, which was countered by a disadvantageous effect during truncation. As expected, this produced frequency trajectories across reproduction and stress tolerance selection that recapitulated the patterns observed in our empirical data (Figure S17). Next, we focused on a series of two-locus scenarios in which SNP A was directionally favoured during expansion with neutral fitness effects during truncation, while SNP B had neutral fitness effects during expansion and then came under directional selection during truncation. We then computed fitness values (empirical selection coefficients) during the first generation of truncation (which represents the single generation (no-recombination) of stress tolerance selection in our experiment) to infer how the relationship between the two SNPs may influence their behaviour across phases. Under scenarios in which the two loci were unlinked, their frequency trajectories were largely independent across phases: SNP A increased systematically during expansion with neutral dynamics during truncation, while SNP B exhibited neutral dynamics during expansion and then systematic increases during truncation (Figure 4; Figures S18 and S19). Under a scenario of high linkage and a net attraction between the favoured allele at each SNP (i.e., the favoured allele at SNP A was non-independently assorted with the favoured allele at SNP B), trajectories were largely correlated, causing empirical selection coefficients to indicate a selective advantage of SNP A during truncation even though the locus was in fact neutral during this phase (Figure 4; Figures S20 and S21). Alternatively, under a scenario of high linkage and net repulsion between the favoured alleles at each SNP (i.e., the favoured allele at SNP A was non-independently assorted with the disadvantageous allele at SNP B), SNP A exhibited a trajectory of fluctuating selection whereby it systematically increased in frequency during expansion and then declined during truncation (Figure 4; Figures S22 and S23). This scenario thus represents a form of haplotype-level antagonistic pleiotropy driven by the orientation of causal alleles and the underlying haplotype structure in the population. Finally, under a scenario in which the attracted and repulsed states of the selected alleles occur at equal probability (i.e., random assortment of alleles between loci), the net-effect of possible linkage patterns produces allele frequency trajectories and empirical fitness values that recapitulate the dynamics observed in the 'unlinked' scenario (Figure 4; Figures S24 and S25).

As we have no prior knowledge of a non-independent assortment of selected alleles in our focal population, the final simulated scenario (independent assortment of advantageous alleles between locus A and B) likely represents the most plausible dynamic occurring in our experiment, should two linked SNPs be under differential selection across selection regimes. Therefore, within the confines of the current data (i.e., not yet knowing the underlying causal loci), we conservatively interpret our observations of reversions in allele frequency trajectories as antagonistic pleiotropy at a single SNP, though recognise the possibility that it could in fact represent antagonistic pleiotropy at the haplotype-level. Quantifying how such haplotype structure could be maintained over long time periods, via either strong selection for the repulsed linkage between selected alleles or some form of recombination suppression (e.g., an inversion), hinges upon resolving the causal loci in this system.

14610248, 2026, 3, Downloaded from https://onlinelibrary.wiley.com/doi/10.1111/ele.70363 by University Of Virginia Claude Moore, Wiley Online Library on [25/03/2026]. See the Terms and Conditions (https://onlinelibrary.wiley.com/terms-and-conditions) on Wiley Online Library for rules of use; OA articles are governed by the applicable Creative Commons License

3.4 | The Emergence of Trade-Offs in Response to Natural Environmental Fluctuations

Our second experiment aimed to quantify whether alleles identified via selection under sustained population expansion in a laboratory setting can predict patterns of adaptation and trade-offs in an outdoor environment, where populations adapt both to changes in population density as well as a suite of additional abiotic variables (Supporting Information; Figure S26; Table S7).

Despite dramatic differences in abiotic conditions between our paired indoor and outdoor mesocosms, we found far greater overlap in SNPs exhibiting signatures of selection than expected by chance (one-tailed hypergeometric test; p-value $<<0.001$; Figure 5A). Furthermore, the dominant direction of selection on selected SNPs was conserved between environments throughout population expansion (Figure 5B; Table S6). Notably, we failed to detect significant statistical overlap using the set of loci identified during the reproduction selection experiment of Experiment 1

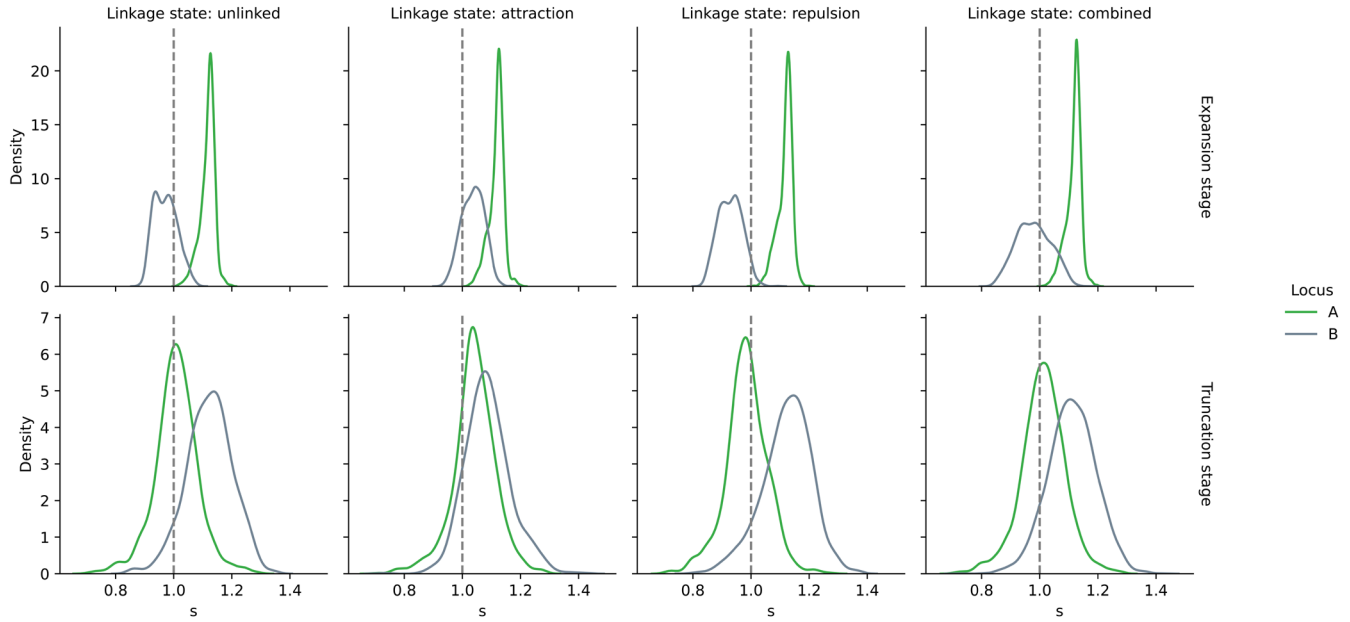

FIGURE 4 | Simulations of multi-locus antagonistic pleiotropy. Kernel density estimates of empirical selection coefficients (s) computed during the first generation of truncation selection in two-locus SLiM simulations ($N = 1000$ simulations per scenario). In each case, the A and B loci are 1 Mb away, with locus A selected during expansion (fitness of favoured allele during expansion = 1.1), but neutral during truncation, while B is neutral during expansion and favoured throughout truncation (fitness of favoured allele during truncation = 1.1). The columns represent different scenarios of linkage between the two loci, whereby 'attraction' represents a scenario in which the favoured alleles at each locus are non-independently assorted with each other, and a state of 'repulsion' represents a scenario in which the favoured allele at each locus was non-independently assorted with the disadvantageous allele at the other locus. The 'combined' scenario represents the average behaviour across linkage scenarios.

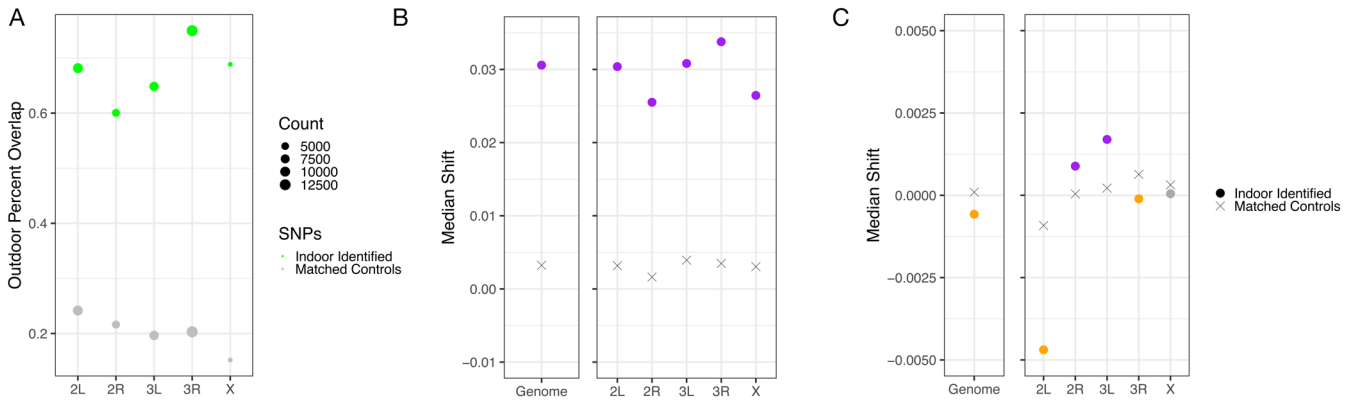

FIGURE 5 | Selection on reproduction under controlled, lab-based conditions predicts patterns of adaptation and trade-offs in a semi-natural mesocosms. (A) Observed vs. expected overlap in SNPs with systematic allele frequency movement (GLM FDR < 0.01; allele frequency change > 2%) in a paired indoor and outdoor experimental evolution study. The amount of overlap of indoor identified SNPs in the outdoor mesocosm was significantly greater than expected by chance for each chromosomal arm (one-tailed hypergeometric test; all p-values $<<0.001$) (B-C) Median shift of alleles identified during expansion in an indoor environment, quantified during population expansion (B) and collapse (C) in an outdoor mesocosm. Coloured circles correspond to indoor-identified SNPs with allele frequency shift distributions that were either significantly greater (orange) or less (purple) than that observed for matched control SNPs (X's) (two-tailed t-test FDR < 0.05).

14610248, 2026, 3, Downloaded from https://onlinelibrary.wiley.com/doi/10.1111/ele.70363 by University Of Virginia Claude Moore, Wiley Online Library on [25/03/2026]. See the Terms and Conditions (https://onlinelibrary.wiley.com/terms-and-conditions) on Wiley Online Library for rules of use; OA articles are governed by the applicable Creative Commons License

with the outdoor mesocosm of Experiment 2 (one-tailed hypergeometric test; p-value > 0.05), likely a result of the distinct inbred reference panels used for each experiment (see Section 4).

We next tested whether this independent, paired indoor-outdoor mesocosm study also revealed the pervasive genome-wide trade-offs quantified in Experiment 1 (Figures 1–4). Specifically, we leveraged an additional month of sampling from the outdoor mesocosm, during which time a population decline and ultimate collapse was observed as winter and the deterioration of abiotic conditions progressed (Bitter et al. 2024). We hypothesized that should those alleles identified in the indoor environment underpin antagonistic pleiotropy and trade-offs for fitness-relevant variation, allele frequencies should reverse in direction as the outdoor mesocosms collapsed. Indeed, we found a significant genome-wide reversion in allele frequencies in the outdoor cages throughout this period, a dynamic primarily driven by patterns of variation on 2L and 3R (Figure 5C; Table S6). Thus, in concert, our two independent experiments provide strong support that seasonal shifts in population density not only underpin patterns of selection observed in natural populations but also elicit trade-offs that preclude the rapid fixation of alleles advantageous in particular ecological contexts.

4 | Discussion

Here, we report data from two experimental evolution studies with large, genetically diverse populations of *D. melanogaster* to quantify genome-wide evidence of fitness trade-offs elicited by ecologically realistic population density fluctuations. In our first experiment, we found that nine generations of sustained population expansion in the absence of density regulation drove parallel, genome-wide shifts in allele frequencies across four, independent replicate populations. The strength of selection coefficients quantified throughout this period (~7% per generation) are comparable to those quantified during sampling individuals of the species between summer and fall from both wild populations and outdoor mesocosms (Bergland et al. 2014; Bitter et al. 2024; Machado et al. 2021; Rudman et al. 2022). Thus, while it has been previously speculated that such patterns of evolution of *D. melanogaster* across seasons may be dominated by adaptation to shifting temperatures (e.g., Boulétreau-Merle et al. 1987), our lab-based manipulation here provides direct evidence that the sole impact of shifting population densities can also drive rapid adaptation over the course of several generations.

By imposing a bout of truncation selection midway through population expansion, during which time individual survival and associated patterns of allele frequency change revealed differences in relative stress tolerance (e.g., desiccation resistance) among genotypes, we quantified a pervasive, genome-wide signal of fluctuating selection. This pattern is indicative of antagonistic pleiotropy, whereby selected alleles conveying advantageous trait values for the phenotypes favoured during reproduction selection convey disadvantageous trait values for the suite of phenotypes favoured during truncation (Connallon and Chenoweth 2019; Curtsinger et al. 1994). Interestingly, at level of larger, structural variants, we found evidence that two major cosmopolitan inversions in the species (In3RP and In3RK) were antagonistically pleiotropic across expansion and truncation. This adds to a growing body of work showing how reduced recombination within inversion breakpoints can give rise to the accumulation of putatively adaptive alleles (Kirkpatrick 2010; Kirkpatrick and Barton 2006; Sturtevant 1921; Sturtevant and Beadle 1936), and the particular importance of these inversions in clinal patterns of variation in geographically widespread populations of *D. melanogaster* (Kapun et al. 2016). It further suggests how such inversions may, over long periods, maintain allelic structure within populations that generate haplotype-level, pleiotropic fitness effects, as we simulated in Results section: *One and two locus simulations of linkage, selection, and antagonistic pleiotropy.* Ultimately, the key implication of the pervasive, genome-wide antagonistic pleiotropy we quantified is that it may maintain variation in the population by precluding the fixation of conditionally advantageous alleles (Curtsinger et al. 1994; Rose 1982; Turelli and Barton 2004; Wittmann et al. 2017). The key challenge for future work is to then discern the underlying causal loci driving these patterns and whether fluctuating selection balances alternate alleles over long time-periods.

It is important to note that those loci with signatures of fluctuating selection identified in Experiment 1 cannot solely be responding to lab-based selection, as the lab environment was held constant across the expansion and truncation phases of the experiment. Still, there may be unquantified aspects of the selective environment beyond strictly fecundity and stress tolerance selection alone that induce phase-specific patterns of selection. Furthermore, it is noteworthy that the timescale over which we evaluated allele frequency behaviour for expansion and truncation differed: expansion occurred across nine discrete generations, while truncation comprised a single generation of desiccation-associated selection. In a natural context, this design mirrors a population at or near carrying capacity that is faced with a pulse abiotic challenge that selects in an extreme manner for stress tolerance, such as a severe drought, heat wave, or severe storm (Baeckens and Donihue 2025). An interesting, and complementary, extension of this work is now to examine how the dynamics quantified here correspond to those in which the timescale of selection is roughly equivalent across contrasting selection regimes.

Our second experiment, which compared observations of allele frequency shifts between indoor (lab-based) and outdoor (semi-natural) mesocosms, demonstrated that selection induced by population size expansion is likely a prominent force driving patterns of adaptation across seasons in natural populations, where shifting population densities occur in concert with a suite of fluctuating abiotic conditions. In effect, this finding indicates that the repeated signals of fluctuating selection quantified across populations and through time (Bergland et al. 2014; Bitter et al. 2024; Machado et al. 2021; Rudman et al. 2022) may be underpinned by fundamental life-history trade-offs that emerge as a result of population boom-bust demographic dynamics. As such boom-bust dynamics are a generic feature of populations across taxa, this phenomenon may thus be more widespread than previously recognised and provide a key instance of the interplay of ecological and evolutionary forces in natural populations (Boor et al. 2018; Carroll et al. 2007; Hendry 2016; Kendall et al. 1999). This predictability of adaptation bolsters an additional hypothesis regarding the nature of the underlying genetic variation: loci responding to rapidly fluctuating selection are not

14610248, 2026, 3, Downloaded from https://onlinelibrary.wiley.com/doi/10.1111/ele.70363 by University Of Virginia Claude Moore, Wiley Online Library on [25/03/2026]. See the Terms and Conditions (https://onlinelibrary.wiley.com/terms-and-conditions) on Wiley Online Library for rules of use; OA articles are governed by the applicable Creative Commons License

specific in their response to particular abiotic parameters, but rather respond more coarsely to generic and repeatable features of the selective environments, in this case the population density fluctuations that occur yearly in the system. Such a 'coarse-graining' of the architecture of the adaptive response could position life-history trade-offs and fluctuating selection as a key force maintaining variation in natural populations.

It is noteworthy that the two separate experiments conducted here revealed distinct genetic architecture of underlying fitness trade-offs in the species. For example, chromosomal arm 2L exhibited strong evidence of antagonistic pleiotropy between population expansion and collapse during our paired indoor-outdoor mesocosm experiment, but was not involved in the trade-offs elicited by the expansion/truncation selection regimes of Experiment 1. Furthermore, we did not detect any shared enrichment of SNPs with evidence of linked selection across Experiments 1 and 2. While there were distinct methodological and environmental differences that may have played a role in this discordance, a more salient driver may be the use of a different inbred reference panels. As our analyses ultimately identify sets of SNPs in tight linkage to an underlying causal locus, differences in patterns of linkage across mapping populations could, in effect, lead to dramatic differences in the relative effect size of marker alleles across studies (Hu et al. 2025). Thus, resolving the specific causal loci underpinning selection in this system is a key future step in resolving how ecological dynamics shape patterns of variation in natural populations of the species.

Author Contributions

The experiment was conceived by D.A. Petrov, P. Schmidt, A.O. Bergland, S. Rajpurohit and M.C. Bitter. Data curation for the population expansion/truncation experimental evolution study was conducted by S. Rajpurohit, N.J. Betancourt, S. Tilk, A.O. Bergland, S. Greenblum and P. Schmidt. Data curation paired indoor and outdoor mesocosm study was conducted by M.C. Bitter, S. Berardi, H. Oken and P. Schmidt. Formal analysis was carried out by S. Greenblum, J.A. Hemker, Egor Lappo, and M.C. Bitter. The original manuscript was prepared by M.C. Bitter, S. Greenblum, P. Schmidt and D.A. Petrov. All authors reviewed and edited the manuscript.

Acknowledgements

We are grateful to members of the Petrov and Schmidt labs for discussion during experimental design, lab work and data analysis. We thank our funding organisations: the National Science Foundation (NSF PRFB 2109407 to M.C. Bitter) and the National Institutes of Health (NIH 5R35GM118165-07 to D.A. Petrov and NIH R01GM100366 and R01GM137430 to P. Schmidt), as well as funding support from the Chan Zuckerberg Biohub.

Funding

National Science Foundation (NSF PRFB 2109407 to M.C. Bitter) and the National Institutes of Health (NIH 5R35GM118165-07 to D.A. Petrov and NIH R01GM100366 and R01GM137430 to P. Schmidt), as well as funding support from the Chan Zukerberg Biohub.

Data Availability Statement

Sequencing data from the DGRP lines used in the population expansion/truncation experiment (Experiment 1) are publicly available at NCBI accession PRJNA36679. Founder line sequences for the paired indoor/outdoor mesocosm study (Experiment 2) are available at NCBI accession PRJNA722305. Raw sequencing reads from pooled samples collected during Experiments 1 and 2 are available at NCBI accessions PRJNA1390176 and PRJNA1031645, respectively. All raw allele frequency data necessary to replicate the results presented here are publicly available on Dryad: https://datadryad.org/dataset/doi:10.5061/dryad.hx3ffbgt1. Code associated with all analyses conducted in this manuscript are publicly available at the following repository: https://doi.org/10.5281/zenodo.18274780.

Peer Review

The peer review history for this article is available at https://www.webofscience.com/api/gateway/wos/peer-review/10.1111/ele.70363.

References

Baeckens, S., and C. M. Donihue. 2025. "Evolutionary Consequences of Extreme Climate Events." *Current Biology* 35: R850–R864. https://doi.org/10.1016/j.cub.2025.07.046.

Band, H. T., and P. T. Ives. 1961. "Correlated Changes in Environment and Lethal Frequency in a Natural Population of *Drosophila melanogaster*." *Proceedings of the National Academy of Sciences* 47: 180–185. https://doi.org/10.1073/pnas.47.2.180.

Battesti, A., N. Majdalani, and S. Gottesman. 2011. "The RpoS-Mediated General Stress Response in *Escherichia coli*." *Annual Review of Microbiology* 65: 189–213. https://doi.org/10.1146/annurev-micro-090110-102946.

Behrman, E. L., and P. Schmidt. 2022. "How Predictable Is Rapid Evolution?" https://doi.org/10.1101/2022.10.27.514123.

Behrman, E. L., S. S. Watson, K. R. O'Brien, M. S. Heschel, and P. S. Schmidt. 2015. "Seasonal Variation in Life History Traits in Two Drosophila Species." *Journal of Evolutionary Biology* 28: 1691–1704. https://doi.org/10.1111/jeb.12690.

Bergland, A. O., E. L. Behrman, K. R. O'Brien, P. S. Schmidt, and D. A. Petrov. 2014. "Genomic Evidence of Rapid and Stable Adaptive Oscillations Over Seasonal Time Scales in Drosophila." *PLoS Genetics* 10: e1004775. https://doi.org/10.1371/journal.pgen.1004775.

Bitter, M. C., S. Berardi, H. Oken, et al. 2024. "Continuously Fluctuating Selection Reveals Fine Granularity of Adaptation." *Nature* 634: 389–396. https://doi.org/10.1038/s41586-024-07834-x.

Boor, G. K. H., C. B. Schultz, E. E. Crone, and W. F. Morris. 2018. "Mechanism Matters: The Cause of Fluctuations in Boom—Bust Populations Governs Optimal Habitat Restoration Strategy." *Ecological Applications* 28: 356–372.

Boulétreau-Merle, J., P. Fouillet, and O. Terrier. 1987. "Seasonal Variations and Balanced Polymorphisms in the Reproductive Potential of Temperate *D. melanogaster* Populations." *Entomologia Experimentalis et Applicata* 43: 39–48. https://doi.org/10.1111/j.1570-7458.1987.tb02200.x.

Carroll, S. P., A. P. Hendry, D. N. Reznick, and C. W. Fox. 2007. "Evolution on Ecological Time-Scales." *Functional Ecology* 21: 387–393. https://doi.org/10.1111/j.1365-2435.2007.01289.x.

Charlesworth, B. 1994. "Evolution in Age-Structured Populations." In *Cambridge Studies in Mathematical Biology*, 2nd ed. Cambridge University Press. https://doi.org/10.1017/CBO9780511525711.

Cole, J. M., C. B. Scott, M. M. Johnson, et al. 2024. "The Battle of the Sexes in Humans Is Highly Polygenic." *Proceedings of the National Academy of Sciences* 121: e2412315121. https://doi.org/10.1073/pnas.2412315121.

Connallon, T., and S. F. Chenoweth. 2019. "Dominance Reversals and the Maintenance of Genetic Variation for Fitness." *PLoS Biology* 17: e3000118. https://doi.org/10.1371/journal.pbio.3000118.

14610248, 2026, 3, Downloaded from https://onlinelibrary.wiley.com/doi/10.1111/ele.70363 by University Of Virginia Claude Moore, Wiley Online Library on [25/03/2026]. See the Terms and Conditions (https://onlinelibrary.wiley.com/terms-and-conditions) on Wiley Online Library for rules of use; OA articles are governed by the applicable Creative Commons License

Curtsinger, J. W., P. M. Service, and T. Prout. 1994. "Antagonistic Pleiotropy, Reversal of Dominance, and Genetic Polymorphism." *American Naturalist* 144: 210–228. https://doi.org/10.1086/285671.

Da Lage, J.-L., P. Capy, and J.-R. David. 1989. "Starvation and Desiccation Tolerance in *Drosophila melanogaster* Adults: Effects of Environmental Temperature." *Journal of Insect Physiology* 35: 453–457. https://doi.org/10.1016/0022-1910(89)90051-6.

Del Monte-Luna, P., B. W. Brook, M. J. Zetina-Rejón, and V. H. Cruz-Escalona. 2004. "The Carrying Capacity of Ecosystems." *Global Ecology and Biogeography* 13: 485–495. https://doi.org/10.1111/j.1466-822X.2004.00131.x.

Flatt, T., G. V. Amdam, T. B. L. Kirkwood, and S. W. Omholt. 2013. "Life-History Evolution and the Polyphenic Regulation of Somatic Maintenance and Survival." *Quarterly Review of Biology* 88: 185–218. https://doi.org/10.1086/671484.

Gleason, J. M., P. R. Roy, E. R. Everman, T. C. Gleason, and T. J. Morgan. 2019. "Phenology of Drosophila Species Across a Temperate Growing Season and Implications for Behavior." *PLoS One* 14: e0216601. https://doi.org/10.1371/journal.pone.0216601.

Haller, B. C., and P. W. Messer. 2023. "SLiM 4: Multispecies Eco-Evolutionary Modeling." *American Naturalist* 201: E127–E139. https://doi.org/10.1086/723601.

Hendry, A. P. 2016. *Eco-Evolutionary Dynamics*. Princeton University Press. https://doi.org/10.1515/9781400883080.

Hiraizumi, Y. 1961. "Negative Correlation Between Rate of Development and Female Fertility in *Drosophila Melanogaster*." *Genetics* 46: 615–624. https://doi.org/10.1093/genetics/46.6.615.

Hoffmann, A. A., and P. A. Parsons. 1989a. "Selection for Increased Desiccation Resistance in *Drosophila melanogaster*: Additive Genetic Control and Correlated Responses for Other Stresses." *Genetics* 122: 837–845. https://doi.org/10.1093/genetics/122.4.837.

Hoffmann, A. A., and P. A. Parsons. 1989b. "An Integrated Approach to Environmental Stress Tolerance and Life-History Variation: Desiccation Tolerance in Drosophila." *Biological Journal of the Linnean Society* 37: 117–136. https://doi.org/10.1111/j.1095-8312.1989.tb02098.x.

Hu, S., L. A. F. Ferreira, S. Shi, et al. 2025. "Fine-Scale Population Structure and Widespread Conservation of Genetic Effect Sizes Between Human Groups Across Traits." *Nature Genetics* 57: 379–389. https://doi.org/10.1038/s41588-024-02035-8.

Ives, P. T. 1945. "The Genetic Structure of American Populations of *Drosophila melanogaster*." *Genetics* 30: 167–196. https://doi.org/10.1093/genetics/30.2.167.

Johnston, S. E., J. Gratten, C. Berenos, et al. 2013. "Life History Trade-Offs at a Single Locus Maintain Sexually Selected Genetic Variation." *Nature* 502: 93–95. https://doi.org/10.1038/nature12489.

Kapun, M., D. K. Fabian, J. Goudet, and T. Flatt. 2016. "Genomic Evidence for Adaptive Inversion Clines in Drosophila Melanogaster." *Molecular Biology and Evolution* 33, no. 5: 1317–1336. https://doi.org/10.1093/molbev/msw016.

Kendall, B. E., C. J. Briggs, W. W. Murdoch, et al. 1999. "Why Do Populations Cycle? A Synthesis of Statistical and Mechanistic Modeling Approaches." *Ecology* 80: 1789–1805. https://doi.org/10.1890/0012-9658(1999)080%255B1789:WDPCAS%255D2.0.CO;2.

Kessner, D., T. L. Turner, and J. Novembre. 2013. "Maximum Likelihood Estimation of Frequencies of Known Haplotypes From Pooled Sequence Data." *Molecular Biology and Evolution* 30: 1145–1158. https://doi.org/10.1093/molbev/mst016.

Kirkpatrick, M. 2010. "How and Why Chromosome Inversions Evolve." *PLoS Biology* 8: e1000501. https://doi.org/10.1371/journal.pbio.1000501.

Kirkpatrick, M., and N. Barton. 2006. "Chromosome Inversions, Local Adaptation and Speciation." *Genetics* 173: 419–434. https://doi.org/10.1534/genetics.105.047985.

Kültz, D. 2005. "Molecular and Evolutionary Basis of the Cellular Stress Response." *Annual Review of Physiology* 67: 225–257. https://doi.org/10.1146/annurev.physiol.67.040403.103635.

Machado, H. E., A. O. Bergland, R. Taylor, et al. 2021. "Broad Geographic Sampling Reveals the Shared Basis and Environmental Correlates of Seasonal Adaptation in Drosophila." *eLife* 10: e67577. https://doi.org/10.7554/eLife.67577.

Mérot, C., V. Llaurens, E. Normandeau, L. Bernatchez, and M. Wellenreuther. 2020. "Balancing Selection via Life-History Trade-Offs Maintains an Inversion Polymorphism in a Seaweed Fly." *Nature Communications* 11: 670. https://doi.org/10.1038/s41467-020-14479-7.

Roff, D. A., and D. J. Fairbairn. 2007. "The Evolution of Trade-Offs: Where Are We?" *Journal of Evolutionary Biology* 20: 433–447. https://doi.org/10.1111/j.1420-9101.2006.01255.x.

Rose, M. R. 1982. "Antagonistic Pleiotropy, Dominance, and Genetic Variation." *Heredity* 48: 63–78. https://doi.org/10.1038/hdy.1982.7.

Rudman, S. M., S. I. Greenblum, S. Rajpurohit, et al. 2022. "Direct Observation of Adaptive Tracking on Ecological Time Scales in Drosophila." *Science* 375: eabj7484. https://doi.org/10.1126/science.abj7484.

Schmidt, P. S., A. B. Paaby, and M. S. Heschel. 2005. "Genetic Variance For Diapause Expression and Associated Life Histories in *Drosophila melanogaster*." *Evolution* 59: 2616–2625. https://doi.org/10.1111/j.0014-3820.2005.tb00974.x.

Service, P. M. 1987. "Physiological Mechanisms of Increased Stress Resistance in *Drosophila melanogaster* Selected for Postponed Senescence." *Physiological Zoology* 60: 321–326. https://doi.org/10.1086/physzool.60.3.30162285.

Stearns, S. C. 1989. "Trade-Offs in Life-History Evolution." *Functional Ecology* 3: 259–268. https://doi.org/10.2307/2389364.

Sturtevant, A. H. 1921. "A Case of Rearrangement of Genes in Drosophila." *Proceedings of the National Academy of Sciences* 7: 235–237. https://doi.org/10.1073/pnas.7.8.235.

Sturtevant, A. H., and G. W. Beadle. 1936. "The Relations of Inversions in the X Chromosome of *Drosophila melanogaster* to Crossing Over and Disjunction." *Genetics* 21: 554–604. https://doi.org/10.1093/genetics/21.5.554.

Tilk, S., A. Bergland, A. Goodman, P. Schmidt, D. Petrov, and S. Greenblum. 2019. "Accurate Allele Frequencies From Ultra-Low Coverage Pool-Seq Samples in Evolve-and-Resequence Experiments." *G3: Genes, Genomes, Genetics* 9: 4159–4168. https://doi.org/10.1534/g3.119.400755.

Turelli, M., and N. H. Barton. 2004. "Polygenic Variation Maintained by Balancing Selection: Pleiotropy, Sex-Dependent Allelic Effects and G × E Interactions." *Genetics* 166: 1053–1079. https://doi.org/10.1093/genetics/166.2.1053.

Wiberg, R. A. W., O. E. Gaggiotti, M. B. Morrissey, and M. G. Ritchie. 2017. "Identifying Consistent Allele Frequency Differences in Studies of Stratified Populations." *Methods in Ecology and Evolution* 8: 1899–1909. https://doi.org/10.1111/2041-210X.12810.

Wittmann, M. J., A. O. Bergland, M. W. Feldman, P. S. Schmidt, and D. A. Petrov. 2017. "Seasonally Fluctuating Selection Can Maintain Polymorphism at Many Loci via Segregation Lift." *Proceedings of the National Academy of Sciences* 114: E9932–E9941. https://doi.org/10.1073/pnas.1702994114.

Zera, A. J., and L. G. Harshman. 2001. "The Physiology of Life History Trade-Offs in Animals." *Annual Review of Ecology, Evolution, and Systematics* 32: 95–126. https://doi.org/10.1146/annurev.ecolsys.32.081501.114006.

14610248, 2026, 3, Downloaded from https://onlinelibrary.wiley.com/doi/10.1111/ele.70363 by University Of Virginia Claude Moore, Wiley Online Library on [25/03/2026]. See the Terms and Conditions (https://onlinelibrary.wiley.com/terms-and-conditions) on Wiley Online Library for rules of use; OA articles are governed by the applicable Creative Commons License

Zhu, J.-K. 2016. "Abiotic Stress Signaling and Responses in Plants." *Cell* 167: 313–324. https://doi.org/10.1016/j.cell.2016.08.029.

Supporting Information

Additional supporting information can be found online in the Supporting Information section. **Data S1:** ele70363-sup-0001-DataS1.docx.csv. **Data S2:** ele70363-sup-0002-DataS2.docx.csv. **Data S3:** ele70363-sup-0003-DataS3.docx.csv. **Data S4:** ele70363-sup-0004-DataS4.docx.csv. **Data S5:** ele70363-sup-0005-DataS5.docx.csv. **Data S6:** ele70363-sup-0006-DataS6.docx.pdf.

14610248, 2026, 3, Downloaded from https://onlinelibrary.wiley.com/doi/10.1111/ele.70363 by University Of Virginia Claude Moore, Wiley Online Library on [25/03/2026]. See the Terms and Conditions (https://onlinelibrary.wiley.com/terms-and-conditions) on Wiley Online Library for rules of use; OA articles are governed by the applicable Creative Commons License